Spring 2020

Glacial Troughs Eject Wind-Driven Shelf Circulation to the Slope

Patrick Hampson
University of New Hampshire, Durham

Glacial Troughs Eject Wind-Driven Shelf Circulation to the Slope

By

Patrick Hampson

MS, University of New Hampshire, 2020

THESIS

Submitted to the University of New Hampshire

in Partial Fulfillment of

the Requirements for the Degree of

Master of Science

in

Oceanography

May 2020

This thesis was examined and approved in partial fulfillment of the requirements for the degree of Master of Science in Oceanography by:

James Pringle, Professor, Earth Sciences

Thomas Lippmann, Associate Professor, Earth Sciences

Gregory Chini, Professor, Mechanical Engineering

On April 24, 2020

Approved signatures are on file with the University of New Hampshire Graduate School.

Dedication

This thesis is dedicated to my beloved Angela, whose steady support enabled me to achieve this degree.

Acknowledgements

I would like to express my gratitude for the careful guidance of my research and writing from James Pringle, whose criticisms encouraged me to grow. I would like to also thank my friends and family, especially my Mother and Father, for their reliable support. Finally, I'd like to express my appreciation for the National Science Foundation grant 1459609 for funding this research.

Table of Contents

Abstract

Glacial troughs are flat-bottomed, steep-sided submarine valleys, which almost or entirely incise the shelf, that significantly alter coastal circulation. A barotropic, linear, steady-state model is used to quantify this alteration as a function of shelf geometry. These model results demonstrate that troughs eject most of the shelf transport offshore to the slope. This offshore ejection diminishes wind-driven alongshore transport downwave of the trough; downwave is the direction of long coastal trapped wave propagation.

Offshore ejection is caused by bottom friction dissipating relative vorticity. Troughs enhance offshore ejection by generating relative vorticity. This is because linear flows on an f-plane (used in this model) follow isobaths to first order. Troughs on the shelf generate relative vorticity through two means: the curving isobaths, which define the trough, steer flows, creating a "flow curvature," and the narrowed shelf, between the coast and trough, accelerates the flow and creates a "flow shear." The relative importance of these two trough-induced mechanisms and a quantification of the net ejection is found with this model.

1 Introduction

Glacial troughs are relatively deep, "u-shaped" submarine valleys that cross most of the shelf. Troughs, which were usually formed by glaciation, are concentrated at high latitudes: the shelves of the Arctic, Southern Ocean, Greenland, Norway, and others (Harris and Whiteway 2011). How troughs modify coastal circulation is understudied in the existing literature. However, research exists on how narrowing/widening shelves and river-carved canyons modify coastal circulation (Pringle 2002; Williams, Gawarkiewicz, and Beardsley 2001; Allen and Hickey 2010; Chapman and Gawarkiewicz 2012). This literature demonstrates that bathymetric control of coastal circulation is important. Extending this type of research to the trough will improve theories of coastal circulation, such as how shelfbreak jets and concentrated slope flows are formed (Chapman 1986; Fratantoni and Pickart 2007; Greatbatch, Pal, and Ren 1995; Greenberg and Petrie 1988; Han et al. 2008).

Modification of shelf circulation by troughs has been observed. Circulation developed throughout the Labrador Sea is modified by the complex bathymetry of the Laurentian Channel; this channel is a significant trough that incises the entire shelf. This modified circulation then flows over the Scotian Shelf in a way that is primarily modified by bathymetry (Sandstrom 1980). Also, on the Norwegian Shelf there exists vibrant ecosystems and distinct sediment distribution patterns; both features have been attributed to the shelf's multiple troughs (Buhl-Mortensen et al. 2012). These observations demonstrate the importance of understanding trough-driven dynamics.

Trough-driven dynamics are modeled here with a barotropic, linear, steady-state model. This model's results will help researchers refine how the Mid-Atlantic Bight is modified by the Laurentian Channel, how wind-driven circulation on the Greenland shelf is altered by its numerous troughs, and other circulation patterns that are impacted by troughs.

Understanding how fjords impact coastal circulation will be improved with these results, as fjords are a limit case of trough bathymetry. Whether fjord bathymetry steers shelf flows

into or away from the coast is found here. Understanding the circulation of these regions aids in predicting glacial mass-balances. This is because fjords often have sea-ice interfaces, whose instabilities depend on which water masses (warm or cold) penetrate onshore to the ice (Straneo et al. 2011).

A trough separates the shelf into two primary study regions: the shelf upwave of the trough, and the shelf downwave. Downwave is the propagation direction of long coastal trapped waves, which travels with shallows on the right in the northern hemisphere (Battisti and Hickey 1984); upwave is the reverse direction. The effect of winds on shelf circulation at any particular alongshore point is due to winds upwave of such flows. At some alongshore point, the structure of a shelf flow is the consequence of all upwave forcing. Therefore, the upwave shelf circulation is unaltered by the trough, whereas the downwave shelf circulation is an adjusted state to the trough impact (Csanady 1978; Pringle 2002). This study determines how a trough modifies an unperturbed upwave flow into an adjusted, downwave flow.

A wind-generated shelf flow is used as the unperturbed, upwave condition. By studying how troughs modify this wind-generated flow into some downwave-adjusted state, we can better understand the interaction between bathymetric and surface forcing on the shelf. Furthermore, downwave winds are also modeled, in addition to this upwave wind-generated flow that has no downwave wind forcing. By including these winds downwave of the trough, this allows for a better understanding of how troughs modify wind-forced shelf circulation.

Wind forcing and subsequent shelf circulation is studied from the downwelling-favorable orientation in this study. Analysis of the results will assume this direction when describing how troughs modify shelf flows. This analysis shows how a trough moves streamlines across isobaths from the shelf to the slope. An equally valid analysis of these results, given the linear nature of this model, shows how troughs can upwell slope flows onto the shelf, in the case of forcing/flows of the opposite orientation. This opposite perspective is explored in the discussion/conclusions.

2 Methods

2.1 The Conceptual Model

Circulation is modeled on an f-plane shelf (constant Coriolis frequency), where the y-axis points alongshore north and positive x-axis points offshore east. This western boundary shelf's bathymetry is defined to include a trough, as seen in figure 1.

Waters on this shelf are assumed to be barotropic, i.e., the Rossby radius of deformation, $\frac{\sqrt{gH}}{f}$ (where g is gravitational acceleration, H is depth, and f is the Coriolis frequency), is small compared to the cross-shore length scale of bathymetry variation (Pringle 2002). Therefore, these results are applicable to either barotropic shelf waters or to barotropic modes of a baroclinic shelf.

Circulation on this shelf is studied in the steady-state limit, which assumes that the flow has fully adjusted to its forcing, and that the forcing itself is steady. Because wind-driven flows are used, the timescale of adjustment is the frictional spin-down time: $\frac{H}{r}$ (Williams and Carmack 2008), where r is the frictional parameter. For the model parameters chosen, this timescale is of O(2-3 days) at the shelfbreak; beyond this timescale, flows are at a fully adjusted steady-state.

Flows are assumed to be linear, or at small Rossby number, i.e., $\frac{u}{fL} << 1$, where u is the velocity of flows and L is its length scale of variation. Because linear flows follow isobaths to first order, a flow convergence occurs at the narrowed shelf between the coast and the trough head. This convergence accelerates the flow towards a nonlinear regime. This model will properly describe flows approaching a linear breakdown. However, the detailed structure of these accelerated flows is not properly described when $\frac{u}{fL}$ is of O(1).

A linear bottom friction is used, which averages over frictional variations at higher frequencies than the assumed steady-state timescale: tides, surface gravity waves, etc. (Csanady 1978; Greenberg and Petrie 1988). This approximation assumes bottom drag

to be directly proportional to the depth-integrated velocity of the geostrophic interior. This is reasonable, given that these waters are both barotropic and at steady-state. Furthermore, the use of a linear bottom friction has replicated observations to first order (Brink and Allen 1978; Lentz et al. 1999; Wright and Thompson 1983). For simplicity,

$$\vec{\tau_{bot}} = \rho_0 r \frac{\vec{U}}{H}, \tag{1}$$

where τ_{bot} is the bottom frictional stress, ρ_0 is the standard density of water, r is the frictional parameter, $\vec{U}$ is the depth-integrated velocity, and H is the depth of water columns.

The aggregate of these assumptions comprises a model that has been explored by various studies (Csanady 1978; Chapman 1985; Chapman 1986; Gordon 1982; Pringle 2002; Sandstrom 1980; Williams and Carmack 2008). They lead to momentum and continuity equations of the following form:

$$-fV = -gH\eta_x + \frac{\tau^x_{top}}{\rho_0} - \frac{\tau^x_{bot}}{\rho_0} \tag{2a}$$

$$fU = -gH\eta_y + \frac{\tau^y_{top}}{\rho_0} - \frac{\tau^y_{bot}}{\rho_0} \tag{2b}$$

$$U_x + V_y = 0, \tag{2c}$$

where U and V are the depth-integrated cross and alongshore transports (Hu, Hv), respectively, f is the Coriolis frequency, g is gravitational acceleration, H(x,y) defines the bathymetry, η is the surface elevation function, $\tau^x_{top,bot}$ and $\tau^y_{top,bot}$ are the offshore and alongshore components of the surface and bottom stresses, respectively, and ρ_0 is the standard density of water.

The use of mass transport streamfunctions, $U = \Psi_y$ and $V = -\Psi_x$, satisfy the continuity equation (2c). Cross-differentiation of the remaining two-dimensional momentum equations leads to the potential vorticity equation (3):

$$0 = J(\Psi, \frac{f}{H}) + \nabla \cdot (\frac{r}{H^2}\nabla\Psi) - \nabla \times (\frac{\tau^{top}}{\rho_0 H}), \tag{3}$$

where J(a,b) is the Jacobian determinant of the partial derivatives of the vector (a,b).

The potential vorticity equation is composed of three terms (in order of appearance in equation 3): 1) the advection of potential vorticity, $\frac{f}{H}$, by Ψ, 2) the dissipation of relative vorticity, $\nabla^2\Psi$, by bottom friction, r, and 3) the generation of potential vorticity by the wind stress curl τ^{top}. The mechanisms that give rise to the modification of shelf circulation by a trough are described by examining this equation. The numerical implementation of this equation into its model form is described in the appendix (6.1).

2.2 Upwave Wind-Generated Shelf Flow

Troughs are forced from the upwave direction because shelf response occurs in the direction of coastal trapped wave propagation (Battisti and Hickey 1984; Csanady 1978). Therefore, in order to isolate the trough's alteration of shelf circulation, an initial set of model runs are conducted where forcing is limited to the shelf upwave of the trough. By neglecting forcing downwave of the trough, the circulation on the shelf downwave of the trough is purely a trough-adjusted state; the response isn't altered by additional forcing.

Winds are modeled by including the third term of the vorticity equation (3), whose form is of alongshore winds over the shelf domain of interest (upwave of the trough in this case). The section succeeding this one outlines how and why an additional set of model runs are conducted where the shelf downwave of the trough is also forced with winds, in addition to the upwave shelf.

The upwave boundary's streamfunction is set to a flow forced by an alongshore uniform wind forcing over an infinite alongshore uniform shelf upwave of the model domain. This shelf velocity, whose solution is a balance of bottom friction and wind forcing, is

$$v = \frac{\tau^y}{\rho_0 r}, \tag{4}$$

where v is the alongshore velocity, τ^y is the alongshore component of the wind stress, ρ_0 is the standard density of water, and r is the bottom friction parameter.

Without wind forcing over the shelf between this upwave boundary and the trough, this wind-generated flow would migrate off its isobaths in the offshore direction (Csanady 1978). Therefore, wind forcing over the shelf is included in this region so that these wind-generated flows maintain their structure. The combination of this upwave wind-generated flow boundary condition, and wind forcing between this upwave boundary and the trough, assures that the trough is forced with an unaltered wind-generated shelf flow.

The downwave boundary condition is set to match the upwave condition in all cases. This assures that the transport that enters through the upwave boundary can exit the domain. This is acceptable because the impact of this downwave condition is confined to within a Stommel distance (approximately 5km for this shelf) upwave of it, leaving the vast majority of the shelf unaltered by the exact choice of downwave condition (Pringle 2002; Stommel 1948). This assertion is defended in the appendix (6.2).

The coastal condition is set to a hard, no-flow wall. This is done by holding the coastal streamfunction to a constant value so that cross-shore transport ($\Psi_y = U$) is equal to zero.

The offshore streamline is also set to the no-flow condition by holding its value to one which is consistent with the transport through the upwave boundary. The rationale of this choice is twofold: 1) open offshore boundaries are unnecessary for this study because the focus is on isolated shelf dynamics, and 2) even if basin-forced flows came through this boundary, they would steer downwave and follow isobaths out through the downwave boundary, without penetrating onto the shelf. Isolation of the shelf from basin circulation is due to the steep continental slope, whose vorticity gradient largely insulates the shelf from offshore forcing (Chapman 1985).

These four boundary conditions are used for all model runs.

2.3 Wind Forcing Downwave of the Trough

The aforementioned model run set, which uses wind forcing only upwave of the trough, isolates the trough's impact on upwave wind-generated shelf circulation. An additional set of model runs are used which include wind forcing over the entire shelf, i.e., upwave, local, and downwave to the trough.

Results from these runs allow for an observation of how far downwave of trough that its impact remains significant. Winds over this downwave shelf will attempt to regenerate shelf circulation. By observing how far alongshore it takes for a thorough regeneration, or a lack thereof, insight is gained as to how far the trough's alteration is of O(1) significance. Whether winds regenerate shelf flows that were altered by the trough immediately downwave of the trough, or if it takes a significant alongshore distance, is found.

The combination of the first set of runs, which have wind forcing only upwave of the trough, and these model runs, which have winds over the entire shelf, gives a complete picture of the trough impact. The former illustrates the structure and significance of trough alteration to wind-generated shelf flows; the latter demonstrates how far alongshore a trough must be considered.

2.4 Scaling Analysis

Given the model's boundary and wind conditions, there are eight parameters that determine the model input: the frictional parameter, the Coriolis frequency, and six geometric shelf parameters (Figure 1). Model runs are initialized by choosing combinations of these parameter values: a baseline run where all parameters are held to their chosen standard value, and variation runs where each parameter is varied over an array of values while the others are held to their standard value (Table 1).

There exists a set of non-dimensional parameter groups which describe a problem's dy-

namics (Price 2003). The number of these parameter groups is determined by subtracting the model dimensions from the defining parameter total:

$$N = P - D, \tag{5}$$

where N is the number of non-dimensional parameter groups, P is the number of defining parameters (eight in this case), and D is the number of dimensions (two in this case: space and time). This gives six non-dimensional parameters groups, which are defined below in the scaling analysis.

The solution to the potential vorticity equation (the satisfying streamfunction) is used in a scaling analysis with these six parameter groups. This is done by quantifying the trough alteration to the upwave wind-generated shelf flow, as a function of the non-dimensional parameter values. This extracts the parameters that are dynamically dominant (Allen and Hickey 2010). The scaling results, which demonstrates how a trough causes shelf circulation to change, are presented in the following section.

The plots that come from this scaling analysis can be used to predict how much any given trough will alter a shelf's wind-driven circulation. However, an extrapolation of these curves to other problems must be done within this model's physical limits.

3 Results

Long coastal trapped waves are the primary mode of transmitting forcing information to downwave waters, being the initiator of flow adjustment. Therefore, a straightforward approach to analyzing how flows adjust in the alongshore direction is by progressing in the long CTW direction (recall that these waves move with shallows on the right in the northern hemisphere (Battisti and Hickey 1984)). The examination of model results in this study is primarily conducted through a downwave orientation, i.e., north to south on this western-boundary northern-hemisphere shelf. An examination of these same results can be done in the reverse (upwave-oriented) because this model is linear. This secondary analysis is described, in addition to the primary upwave-oriented analysis, in the discussion section. It is shown in this upwave-oriented analysis how troughs can enhance the "absorption" of slope flows onto the shelf through upwelling.

3.1 Bottom Friction Moves Streamlines Across Isobaths

In order to understand how streamlines cross isobaths, two model runs are presented here of trough-less shelves: one with and one without bottom friction (Figure 3). Both shelves are forced with upwave wind-generated shelf flows and were constructed with baseline-value input parameters (Table 1). These model results demonstrate how bottom friction is the mechanism responsible for moving flows across isobaths. Later sections will outline results that build upon this simpler explanation of cross-isobath migration of streamlines, to explain how troughs alter shelf circulation.

For both runs, wind forcing does not exist within the domain, i.e., the third term of the vorticity equation (3) is set to zero. Therefore, the advection of potential vorticity, $J(\Psi, \frac{f}{H})$ is balanced by the dissipation of relative vorticity by bottom friction, $\nabla \cdot (\frac{r}{H^2} \nabla \Psi)$. This balance's resulting streamlines are plotted on the left panel of Figure 3. A further reduction,

where bottom friction is set to zero, is plotted on the right panel. The vorticity equations of these two cases are as follows:

$$0 = \nabla \cdot (\frac{r}{H^2}\nabla\Psi) - J(\Psi, \frac{f}{H}) \tag{6a}$$

$$0 = J(\Psi, \frac{f}{H}), \tag{6b}$$

where (6a) applies to the left panel of Figure 3, and (6b) applies to the right panel.

The contrast between these two cases demonstrates that friction is the mechanism responsible for moving streamlines across isobaths. In the case without bottom friction (right panel), streamlines remain on lines of $\frac{f}{H}$; these are simply isobaths on this f-plane. In the case with bottom friction (left panel), streamlines move across isobaths, offshore to the slope. This offshore migration occurs because of the Arrested Topographic Wave (hereafter ATW) effect, which acts when the alongshore length scale is much larger than the cross-shore scale (Csanady 1978). This ATW-driven offshore migration of streamlines occurs because of bottom friction. Bottom friction acts against the direction of the currents, which in turn drives an offshore bottom Ekman transport. How troughs modify shelf circulation through the mechanism of offshore migration via bottom friction is described below.

3.2 Trough Ejection Mechanisms

Bottom friction acts to move shelf flows, which encounter trough bathymetry, across isobaths. This is illustrated with two model runs: one shelf without a trough, and one with a trough (Figure 4). Like the previous section, input parameters are set to their baseline values (Table 1), but a downwave-oriented wind forcing is used in addition to the wind-generated inflow. Flows that enter through the upwave boundary are maintained with this downwave-oriented wind forcing over the shelf, located upwave of the trough. No winds exist at or downwave

of the trough, allowing for an examination of the trough impact alone. In the model run without a trough on the shelf, the alongshore extent of wind forcing is identical to the forcing used in the trough-shelf case; this allows for direct comparison of the trough impact. A quantification of how much shelf transport is moved offshore to the slope is done for both of these runs.

Figure 4 demonstrates how troughs alter wind-generated shelf circulation. The left panel shows how streamlines on a trough-less shelf evolve in the alongshore, following the ATW dynamic. Downwave of the red transect, where there is no wind forcing, streamlines begin to drift offshore towards the slope. This migration of streamlines towards the slope is greatly increased in the case of a trough, as seen in the right panel. Enhanced offshore migration of shelf flows to the slope by the trough will be referred to as "ejection."

An ejection metric is defined as the percentage of shelf transport lost offshore beyond the shelfbreak across a trough. This is done by comparing how much transport passes through the downwave (black) transect versus how much initially passes through the upwave (red) one:

$$E_{trough} = \frac{\Psi_{shelfbreak,downwave}}{\Psi_{shelfbreak,upwave}} * 100 - E_{notrough}, \tag{7}$$

where E_{trough} quantifies the percentage of shelf transport lost offshore to slope, by comparing the initial amount ($\Psi_{shelfbreak,upwave}$) to the resulting amount ($\Psi_{shelfbreak,downwave}$). Additionally, $E_{notrough}$ quantifies shelf transport loss, but for a shelf without a trough. By subtracting off this value found for a trough-less shelf, this normalizes trough results as "additional" ejection values beyond the trough-less ATW case.

An additional 62% of shelf transport is ejected offshore to the slope in the case of the baseline-parameter trough on the shelf (right panel). Both this ejection result and the visual evolution of streamlines throughout this trough-shelf system indicates that troughs increase the cross-isobath migration of flows to the slope, all the while sharpening an often-observed shelfbreak jet (Chapman 1986; Gawarkiewicz and Chapman 1991).

Enhanced offshore ejection of shelf circulation to the slope is caused by the trough modification of flows from upwave. Upon encountering the trough from the upwave direction, flows steer onshore around the trough, are squeezed into the "narrowed" shelf, and then are ejected offshore to the slope. Flows are attempting to follow isobaths throughout this progression because linear flows follow isobaths to first order (Csanady 1978). Because bottom friction is the mechanism responsible for moving streamlines across isobaths in this linear case, and because troughs enhance net offshore ejection, troughs must somehow intensify the bottom friction mechanism.

Streamlines cross isobaths because bottom friction dissipates relative vorticity. There are two sources of relative vorticity as this flow progresses around/through the trough. The first source is from the steering flows around the trough's curving isobaths. Steering of the flow field along these isobaths creates a flow curvature, i.e., relative vorticity. The second source is of the flow convergence through the narrowed shelf (between the coast and the trough head). This flow convergence causes an acceleration and, in turn, a cross-shore velocity shear, i.e., relative vorticity. These two trough-induced vorticity sources will hereafter be referred to as the curvature and narrowing sources, respectively.

Upon introducing relative vorticity through these two sources to these shelf waters, bottom friction will act to dissipate such vorticity, and streamlines will cross isobaths. These two vorticity sources are depicted with cartoon arrows in figure 5.

The next section explores results of model runs where the input parameters are varied. The ejection metric is quantified for each run case, and a scaling analysis is conducted. This analysis allows for an understanding of the relative contributions of these two vorticity sources to net offshore ejection.

3.3 Relative Contributions of the Curvature and Narrowing Sources to Offshore Ejection

In order to quantify the relative contributions of the curvature and narrowing sources to offshore ejection, variation runs are examined here. Input parameters of these model runs were constructed by varying a single parameter at a time, while holding all others to their baseline values (Table 1). Streamfunction solutions of these variation runs are then used to quantify offshore ejection of shelf flow as a function of non-dimensional parameter groups (Price 2003). As described above, these ejection metric results for trough cases are calculated as "additional" offshore ejection (equation 7), beyond the background shelf transport loss caused by the ATW-dynamic of a trough-less shelf (Csanady 1978). Recall that the trough-less shelf run with baseline input parameters caused a shelf transport loss of 22% (Figure 4).

Scaling analyses extract the relative dominance of parameters on circulation dynamics (Allen and Hickey 2010). In this case, the ejection scaling curves, which plot the dynamic change (ejection) versus the parameters, demonstrates whether the outcome is affected by a changing parameter. Therefore, this scaling analysis is used to quantify the relative strength of the curvature and narrowing (shear) vorticity sources to offshore ejection. The stronger the relation between ejection and a parameter related to one of the vorticity sources, the more that that source contributes to trough ejection. See Figure (1), which introduced the bathymetric schematic of this model, for the relevant parameters used for scaling these two vorticity sources.

The narrowing (shear) source is scaled with two parameter groups: $\frac{L_{head}}{L_{shelf}}$, and $\frac{W_{trough}}{L_{shelf}}$, where L_{head} is the offshore distance of the narrowed shelf, L_{shelf} is the offshore distance of the entire shelf, and W_{trough} is the alongshore distance of the trough's base (Figure 1). The first parameter group ($\frac{L_{head}}{L_{shelf}}$) measures the strength of the narrowing source's mechanism, i.e., flow shear. The narrower the distance between the trough and the coast, the stronger

the shear will become. As the narrowed shelf becomes wider until the trough disappears to the slope, this shear effect will become negligible. The second parameter group ($\frac{W_{trough}}{L_{shelf}}$) measures the accumulation of this shear effect. A trough which spans a longer alongshore distance creates a longer distance for the shear effect to accumulate, whereas a trough width that disappears to zero gives no distance, and therefore, no accumulation of the shear effect. Variation results are shown of enhanced offshore ejection as a function of these two parameter groups (Figure 6).

The left panel plots the first parameter group of the narrowing source ($\frac{L_{head}}{L_{shelf}}$), i.e., shear strength. As the parameter reaches one, the trough disappears to the slope. As this narrowed shelf approaches the total shelf width, the additional ejection caused by the trough reduces to zero, confirming that the trough-less shelf converges to the ATW value. For small values of $\frac{L_{head}}{L_{shelf}}$, the trough approaches a total intersection of the shelf. A full shelf intersection leads to an additional 60% of the shelf flow being ejected offshore to the slope.

The right panel plots the second parameter group for the narrowing source ($\frac{W_{trough}}{L_{shelf}}$), i.e., shear accumulation. As the parameter approaches unity, the alongshore trough width becomes the same distance as the entire shelf width (120 km), and an additional 70% of the shelf flow is ejected to the slope. Because a wider trough increases the accumulation of the shear effect, we see that this parameter is directly proportional to ejection. As the parameter goes to zero, the trough disappears, and ejection converges to the background ATW value. Both of these narrowing source parameter groups change offshore ejection by 60-70% for an O(1) change in parameter.

The curvature source is scaled with the following parameter group: $\frac{W_{wall}}{L_{head}}$, where W_{wall} is the alongshore distance of the trough walls (Figure 1). This parameter group correlates to the significance of isobath curvature. As the trough walls' alongshore distance increases, the wall gradient decreases, reducing the sharpness of isobath curvature. A shorter alongshore distance corresponds to cliff-like walls, i.e., sharper isobath curvature. Therefore, we expect ejection to be indirectly proportional to this parameter because sharper isobaths will increase

the curvature source's contribution.

Figure 7 shows results of the enhanced offshore ejction as a function of this curvature parameter. Indeed, ejection is reduced as the parameter increases because the walls' alongshore distance gets larger, decreasing isobath curvature. This reduction in the curvature source's contribution to ejection with increasing alongshore trough wall distance is because more gradual isobaths reduce the significance of flow curvature. Inversely, as the alongshore distance of the trough walls decreases, offshore ejection increases because isobath curvature becomes more significant. Unlike the narrowing source's scaling, an O(1) change in this curvature parameter causes only a 10% change in offshore ejection (versus 60-70%); this is about one-sixth to one-seventh that of the narrowing source's scaling.

Scaling analyses of results from these variation runs allow for two succinct conclusions: 1) the narrowing and curvature sources cause trough-enhanced offshore ejection of shelf flows to the slope, and 2) the narrowing source dominates these ejection dynamics by a factor of O(5) over that of the curvature source's contribution.

All the previously explored results were forced with winds only upwave of the trough (or the equivalent location in the case of a trough-less shelf). This approach allowed for an isolated understanding of how troughs modify wind-driven shelf circulation. A few conclusions can be made about this impact: 1) troughs enhance the offshore ejection of shelf circulation to the slope, beyond the background ATW amount, 2) this occurs because troughs generate relativity vorticity, which friction dissipates and causes cross-isobath migration, via curvature and narrowing sources, and 3) the narrowing source contributes to ejection more than the curvature source by a factor of O(6-7).

3.4 Alongshore Response Scale of Wind Forcing vs Trough Ejection Impact

Wind forcing over the shelf acts to mitigate the enhanced offshore ejection of shelf transport to the slope caused by a trough. The alongshore scales of both the trough-induced offshore

ejection and shelf response to wind forcing determines how these two phenomena interact. This interaction is determined in this section by examining model results on a shelf which is four times longer than earlier model runs, i.e., 2000 km instead of 500 km. Two runs are examined of this longer shelf: one with a single trough near the upwave boundary, and one with two troughs separated across the alongshore expanse of the shelf. Previously examined runs constrained wind forcing only upwave of the trough, which allowed for an isolation of the trough impact. Instead, these runs use winds downwave of the trough, from the upwave to the downwave boundary.

Figure 8 shows results of these downwave wind cases, with a one-trough run shown on the left and a two-trough run shown on the right. The ejection metrics are normalized against the resulting ATW offshore ejection of this 2000 km shelf without a trough, so that these results are of ejection beyond that standard value. The cross-shore transects used to calculate this change in shelf transport were placed upwave of the first trough and near the downwave boundary. This large separation allows for an understanding of how the trough impact evolves far away from the trough itself. The one-trough case shows a 9% enhanced offshore ejection of shelf transport to the slope at an alongshore distance of approximately 1500 km downwave of the trough. This demonstrates that the trough ejection is largely "forgotten" by this point downwave of the trough, because the wind forcing over the shelf is regenerating the flows. The two-trough case shows a 44% enhanced offshore ejection of shelf transport to the slope. Winds largely regenerated the shelf flows lost by the upwave trough over this 1500 km distance, before shelf flows are once again largely ejected offshore because of the downwave trough.

There is a significant difference between circulation response to wind forcing versus the trough ejection impact. After the initial ejection caused by the upwave trough winds start to regenerate flows on the shelf, acting as a mitigator to the trough ejection impact. However, the alongshore scales of these two responses are vastly different. These model results demonstrate that trough ejection is acting on an alongshore scale of O(10's km). Wind

forcing, however, acts on an alongshore scale - corresponding to how far in the alongshore it would take winds to fully establish shelf circulation - that scales as: $L_{fric} = -\frac{Hf}{2r}L^x$, where L^x is the offshore length scale (Chapman 1986; Pringle 2002). At the shelfbreak, which is the relevant offshore length scale for considering the entire shelf's circulation state, this frictional scale is O(1500 km). Trough ejection is acting on a much shorter length scale than wind response; the ejection scale is approximately 1% that of the wind scale. Therefore, determining whether the trough ejection impact should be considered when modeling some local shelf flows, one must determine how far upwave is the nearest trough. The discussion section will further elaborate the implications of these model results, which show this vast difference in alongshore scale between wind forcing and trough ejection.

3.5 Troughs Enhance Upwelling of Slope Waters to the Shelf

An upwave-oriented wind forcing will produce currents that move upwave. This upwave-oriented configuration is opposite to the results examined thus far, where wind forcing over the shelf is pointed downwave and, in turn, cause shelf flows to move downwave. Because this model is linear, the previously examined results also describe flows oriented in the upwave direction. Therefore, this section will analyze the results in the opposite perspective to before, i.e., a forcing directed upwave that causes flows to move upwave.

Figure 9 shows slope currents moving northwards (upwave) because of winds that blow upwave. The presence of the trough causes these slope flows to cross isobaths, moving onshore to shallower isobaths. The interaction of the slope currents with the trough bathymetry is constrained to streamlines on the slope that are at or shallower than the deepest trough isobath. This can be seen in the figure, where streamlines on the slope offshore of that depth are only slightly altered by the trough. This demonstrates that slope flows deeper than a trough's deepest depths will be unaltered by the trough for this system.

This progression of slope flows that move onshore to the shelf because of the trough is the

reverse case of that which was examined previously. Because the results from the offshore ejection impact is used here to describe an upwelling-favorable case, the dynamics are the same. The curvature and narrowing sources must introduce relative vorticity to these slope currents, which friction will dissipate, causing an adjusted state of flows that end up on the shelf. Whereas the downwelling-favorable case was described as a trough "ejection" impact, this upwelling-favorable progression can be thought of as a trough "absorption" impact. This baseline-parameter trough absorbs slope transport to the shelf, resulting in a 53% change in shelf transport, as compared to the transport on the shelf downwave of the trough.

Recall that forcing is communicated via propagation of coastal trapped waves, which move with shallows on the right in the northern hemisphere (southwards for this western-boundary shelf). This remains true for both upwelling-favorable and downwelling-favorable cases. Whether winds are oriented upwave or downwave, only the waters downwave of these winds will adjust to the forcing because of the asymmetric communication of the forcing. Therefore, the scaling results that demonstrated how far downwave of a trough its impact must be considered, are equally valid for forcing/flows of either downwave or upwave orientation.

4 Discussion

4.1 Trough-Enhanced Downwelling of Shelf Flows to the Slope, and its Implications

Shelf currents that move downwave (in the direction of coastal trapped waves) are largely ejected offshore to the slope by troughs (Figure 4). These flows, which were forced by downwave-oriented winds over the shelf, encounter the trough and attempt to navigate around it because linear flows follow isobaths on this f-plane. Upon navigating around/through this trough bathymetry, relative vorticity is generated and introduced to the system. Bottom friction works to dissipate this relative vorticity, and in turn, causes the migration of shelf flows off their isobaths to deeper waters. This migration occurs through a downwelling Ekman bottom transport. The net effect is that shelf transport is ejected offshore to the slope.

There are two sources of relative vorticity due to these linear flows following the trough isobaths: 1) curvature, and 2) narrowing. The scaling analysis revealed that the narrowing source dominates the ejection dynamics by a factor of O(6-7) greater than that of the curvature source's contribution. Therefore, the trough parameters that most control ejection of shelf flows are the alongshore width, and the distance between the trough head and the coast. A trough that intersects most of the shelf, and extends a large alongshore distance, will make a more significant impact on coastal circulation than one which is narrow in the alongshore, and resides far offshore. A trough which exhibits this geometry, and indeed drastically alters coastal circulation, is the Laurentian Channel. The southward-moving flows from the Labrador Sea are swiftly ejected offshore to slope, resulting in a sharp boundary of different shelf circulation types at this bathymetric boundary (Dever et al. 2016). The opposite case to this is bathymetric features which are narrow and far offshore, i.e., outlier river-carved canyons that incise a portion of shelf. Although these canyons do impact coastal circulation, their impact is lesser and of a different nature to that the trough impact (Allen

and Hickey 2010). It is only when canyons cut across much of the shelf that their impact on shelf circulation becomes consequential; the Hudson Canyon is an example of such an exceptional river-carved canyon (Zhang and Lentz 2017).

There are multiple secondary effects on ocean dynamics due to this trough ejection of shelf transport to the slope. Because troughs cause shelf circulation to migrate offshore to the slope this will enhance a shelfbreak jet, which is often observed (Fratantoni and Pickart 2007; Greatbatch, Pal, and Ren 1995; Greenberg and Petrie 1988; Han et al. 2008). The enhancement of strong currents at the shelfbreak may add to the insulation of the shelf from basin-scale dynamic (Chapman 1985). Additionally, the exchange of shelf waters to the slope by a trough will impact the chemical compositions of both sets of waters. Shelf waters are home to significant biological communities and physical exchange properties. Therefore, because troughs downwell shelf waters to deeper depths along the slope, this mechanism should be considered as it relates to exchange of properties between the shelf and ocean basins. For example, the exchange of carbon through this downwelling will contribute to the global carbon cycle (Holt, Wakelin, and Huthnance 2009). Any other secondary phenomenon which would be impacted by the downwelling of shelf waters should consider the role of troughs, especially at higher latitudes where troughs are concentrated.

4.2 Trough-Enhanced Upwelling of Slope Flows to the Shelf, and its Implications

Because this model is linear, the previously used results can be used to examine a downwelling-favorable case, where upwave-oriented winds cause flows to move upwave, i.e., the same pattern explored above, but with reversed flows. Figure (9) represents this upwave-oriented (northward on this western boundary shelf) wind forcing with a white cartoon arrow. Upon encountering the trough, these slope flows are forced to navigate through the trough bathymetry. Subsequently, these flows end up on the shelf after migrating through this trough region. The adjusted state is of an increase of shelf transport by 53% upwave of the trough, compared

to the lack of shelf transport downwave of the trough. This is simply the reverse situation to that of the downwelling-favorable case, where shelf flows are ejected offshore to the slope.

Flows on isobaths at or shallower than the trough's deepest isobath are upwelled onto the shelf. The most-offshore streamline plotted, which resides on a slope isobath at a depth where the trough merges into the slope, is only slightly altered as it navigates through the trough region. This demonstrates that a trough will only impact slope currents that run along isobaths at least as shallow as the deepest isobaths of the trough. For the trough to upwell flows of a depth deeper than its own, some other mechanism must first migrate flows to the relatively shallower trough-depth.

The trough's impact on these upwave-moving slope currents is the exact opposite as that of the offshore ejection phenomenon. The difference is that for this upwelling-favorable case, the trough increases the amount of transport on the shelf by moving slope currents to the shelf: "absorbing" them. In light of this trough-induced absorption, two conclusions can now be made in total about a trough's impact on coastal circulation: 1) a trough will cause downwave-moving shelf flows to eject offshore to the slope through downwelling, and 2) a trough will cause upwave-moving slope flows to absorb onshore to the shelf through upwelling.

This upwelling-favorable situation is only relevant to upwave-moving flows. In the case of steady-state upwave-moving currents, there must be some forcing, located upwave of such flows, that is oriented upwave as well. Shorter timescale forcing of winds, such as storms, can induce flows to move upwave on this timescale. For example, winter storm winds over the New England Shelf drive circulation in an orientation opposite of the annual mean (Beardsley and Haidvogel 1981). Therefore, this upwelling by a trough (just like downwelling) can manifest on a shorter timescale than the steady-state scale described throughout this study.

The upwelling of flows onto the shelf will have substantial impacts on ocean dynamics. For example, warm slope waters that upwell via a trough into the Amundsen Sea account for most of the heating, and subsequent basal melting, of the entire West Antarctic Ice

Shelf region (Walker et al. 2007; Wåhlin et al. 2013). Additionally, the troughs along the Greenland Shelf significantly contribute to both nutrient cycling within those local coastal waters (Cape et al. 2019), and ice melt (Rysgaard et al. 2020). Both the exchange of heat and nutrients between the shelf and deeper waters through a trough are first order ocean dynamics; dynamics which impact glacial-mass balances, biological populations within coastal waters, etc. The combination of upwelling of slope waters to the shelf, and steering of such flows between the trough head and the coast through the trough narrowing mechanism, enhances the presence of slope waters onshore of the trough. Because this fjord location may likely contain a glacial tongue, this mechanism could largely contribute to glacial melt. Additionally, troughs upwelling deeper waters onto the shelf could largely contribute to biological processes, because of deeper waters being rich in nutrients.

Although the literature attributes these observations of trough-induced upwelling to buoyancy forcing, this study demonstrates that troughs can cause upwelling even in the unstratified limit. Therefore, observations of trough-driven circulation patterns shouldn't be reduced to buoyancy forcing alone. Barotropic dynamics must be accounted for.

4.3 How Far Alongshore Does the Trough Impact Remain Significant?

The trough ejection and absorption impacts will be first-order effects on coastal circulation within the alongshore trough-response scale of a trough. This was demonstrated by this model's baseline-parameter trough, which caused an O(50%) change in shelf transport. The alongshore scaling of these trough dynamics, as compared to that of wind forcing, demonstrates that the trough impact will remain relevant for hundreds of kilometers downwave of the trough. Whereas the trough ejection/absorption impact acts on an alongshore scale of O(10s km), the alongshore scale of wind response is known to be: $L_{fric} = -\frac{Hf}{2r}L^x$ (Chapman 1986). The appropriate depth scale for H to understand shelf adjustment is the shelfbreak depth. The appropriate offshore length scale for L^x is the shelf width. Therefore, it can

be concluded that a shelf with a shallower shelfbreak depth and a narrower offshore extent, will have a shorter alongshore scale of adjustment to wind forcing. For shelves with this structure, the trough impact will remain relevant for a lesser alongshore distance downwave of the trough, because the shelf will more quickly adjust to wind forcing. Inversely, a wide shelf with a deep shelfbreak depth will be subject to the trough impact for a longer distance downwave of trough. The other two parameters that drive this alongshore response scale are f, the Coriolis frequency, and r, the bottom frictional parameter. The trough impact will remain significant for longer alongshore distances at high latitudes, when considering that f increases with higher latitude. Finally, stronger linear bottom friction (greater frictional parameter r) will decrease the alongshore distance that the trough impact remains significant because it is inversely proportional; the frictional parameter r is typically $2 - 5 * 10^{-4} \frac{m}{s}$ (Williams and Carmack 2008).

The results of a back of the envelope calculation of the alongshore wind response scale (L_{fric}) for three specific shelves are considered: that of the Scotian Shelf, the shelf along southwestern Greenland, and the Antarctic Shelf directly south of Africa. Appropriate Coriolis frequency values were chosen for each, as well as a frictional parameter value of $5 * 10^{-4} \frac{m}{s}$, and a shelfbreak depth of 100 m. The Scotian Shelf, with a width of approximately 150 km, has an alongshore response scale of O(1,500 km), the southern Greenland Shelf, with a width of approximately 40 km, has an alongshore response scale of O(500 km), and the Antarctic Shelf near 15°E, with a width of approximately 10 km, has an alongshore response scale of O(100 km). These three cases show that the alongshore extent of the trough impact can vary wildly depending on a shelf's bathymetry. This scale is a guide to the extent of a trough's influence.

In addition to considering this alongshore scale, which depends on a shelf's parameters, a consideration of the frequency of troughs should be accounted for. Every time flows encounter some trough, it is subject to the trough's impact. The most recent trough encountered by flows is the trough that sets the alongshore scale of relevance. Therefore, upon considering

how far the extent of a trough-driven impact on shelf flows is, one must consider the most nearby trough in the upwave direction.

Shelves with more troughs will be subject to these trough impacts more significantly. Streamlines are more tightly constrained to isobaths at high latitudes because of the stronger Coriolis parameter (f), and troughs exist in higher abundance on glaciated/previously-glaciated shelves at these high latitudes (Harris and Whiteway 2011). Therefore, troughs will be an even greater inhibition on wind-driven circulation on high-latitude shelves.

4.4 Where Does the Model Fail?

Results from this model demonstrate that troughs enhance the ejection of downwave-moving shelf transport to the slope (and enhance the absorption of upwave-moving slope waters to the shelf). Extrapolation of these results to shelf systems can only be done if the system resides within this model's physical regime. The following reiterates the physical limits of this model and describes how to apply these results within these limits.

This model is of coastal flows in the steady-state limit, which depends on the underlying forcing being at a steady-state. Rather than describing the dynamics of adjustment as flows respond to some changing forcing, these results describe how that adjusted state behaves. If a wind forcing changes against what was previously steady, such as a winter storm forcing differently than the seasonal average, then the flows will start to adjust to this new forcing. If this forcing remains stable for a long enough time for the flows to adjust into a steady-state, then these results will once again become relevant. The time scale to determine if flows have reached a steady-state after adjusting to a forcing is the frictional spindown time: $\frac{H}{r}$, where H is the depth of a water column, and r is the frictional parameter (Williams and Carmack 2008). In order to understand the timescale for an entire shelf to adjust, an appropriate choice of H is the shelfbreak depth. The choice of frictional parameter, r, must be chosen as an empirically representative value of a shelf system of interest. Recall that this

frictional parameter is typically in the range of $2 - 5 * 10^{-4} \frac{m}{s}$ (Williams and Carmack 2008). For example, a shelf with a shelfbreak depth (H) of 100 m and a frictional parameter (r) of $5 * 10^{-4} \frac{m}{s}$, the frictional spindown time is $2 * 10^5 s$ or approximately 2.3 days. Therefore, flows on a shelf of this nature will fully adjust to a steady-state in response to some forcing (given that the forcing itself remains steady over this timescale) in about two days.

Barotropic dynamics are described with these model results, allowing for an extrapolation to either barotropic waters or barotropic modes of baroclinic waters (Brink 2006). This limit assumes that the Rossby radius of deformation ($\frac{\sqrt{gH}}{r}$) is small compared to the cross-shore length scale of bathymetry variation (Janowitz and Pietrafesa 1982). The barotropic Rossby radius of deformation varies from approximately 20 km near the coast (at the 10 m isobath) to approximately 60 km at the shelfbreak (using the 100 m isobath). These deformation scales are smaller than the relevant cross-shore length scales, i.e., 30 km from the coast to the trough head, and 150 km for the full shelf, respectively. However, the deformation scale approaches the cross-shore length at the trough location, demonstrating that this is a location where the details of this barotropic model reach its limit. An investigation of the stratification of a coastal system must be conducted to understand whether these barotropic results apply. A climatological analysis of the flows along the western North Atlantic showed how stratification widely varies with seasonal variation of freshwater influx, heating, mixing, and ice coverage (Fratantoni and Pickart 2007). Therefore, applying these barotropic insights becomes more applicable as stratification decreases in the winter.

The final core limit of this model is that these shelf flows are linear. This occurs when the Rossby number is small: $\frac{u}{fL} << 1$. The Rossby number at the upwave boundary of this model, based on the 10 $\frac{cm}{s}$ inflow over a 150 km wide shelf, is approximately 0.006, i.e., strongly linear. The Rossby number begins to increase in this system where the shelf flows are constricted into the narrowed shelf, between the trough head and coast. Flows are accelerated to a magnitude of approximately 30 $\frac{cm}{s}$ across this 25 km shelf (in the case of baseline input parameters), giving a Rossby number of 0.12, i.e., approaching a nonlinear

scale. In the variation run results, where the offshore distance to the trough head was varied, the Rossby number greatly increases as the trough extent goes to the coast. A 1 km wide narrowed shelf, where the trough essentially merges with the coast, gives a Rossby number of 3. For this system, the details of the flow structure are not properly accounted by this linear model. Therefore, currents of significant magnitude over significantly narrow shelves are better described by nonlinear studies. An examination of nonlinear circulation in the Arctic demonstrated how cross-shore exchange between the shelf and the slope occurs in this nonlinear regime (Williams, Gawarkiewicz, and Beardsley 2001).

5 Conclusions

Much of the current understanding of coastal circulation dynamics comes from studying baroclinic dynamics and/or wind forcing (Csanady 1978; Pringle 2018), as well as dynamics associated with river-carved canyons (Allen and Hickey 2010). The contributions of glacial troughs to coastal circulation dynamics has been largely overlooked, despite observations indicating their significance (Buhl-Mortensen et al. 2012; Cape et al. 2019; Wåhlin et al. 2013; Walker et al. 2007). Model results explored in this study affirm that troughs significantly impact coastal circulation dynamics. Although troughs may drive the exchange between the slope and shelf through baroclinic processes, as demonstrated by these cited studies, this model demonstrates that the exchange can occur within the barotropic limit.

Troughs enhance the offshore ejection of barotropic shelf flows to the slope during downwelling-favorable downwave flows (and onshore absorption during upwelling-favorable upwave flows) by generating relative vorticity, which bottom friction dissipates and causes cross-shore migration of currents. Relative vorticity is generated because linear flows navigate around the trough, attempting to maintain their isobaths. This study identified two sources of relative vorticity: curvature (relative vorticity of flows steering around the trough) and narrowing (relative vorticity of accelerated flows between the trough and coast). A scaling analysis demonstrated that the narrowing of isobaths by the trough contributes to offshore ejection by a factor of O(5) more than that of the curvature of isobaths. Therefore, there are two trough dimensions that will most dictate the strength of its impact on coastal circulation: alongshore trough width, and offshore expanse of the trough across the shelf.

Finally, this model characterized how far downwave these trough dynamics remain significant by contrasting its alongshore response scale to that of wind forcing (calculated with the frictional distance, as described in the description section). This trough impact distance can range from O(100 km) on narrow shelves like parts of the Antarctic to O(1500 km) on wide shelves like the Scotian. This alongshore distance should be measured in relation to

the closest trough upwave of some waters of interest.

The cross-shelfbreak exchange of flows driven by a trough can dominate cross-shelfbreak exchange local to and downwave of such trough. This enhanced exchange will greatly modify processes that depend on the exchange of flows between the shelf and slope. For example, troughs downwelling shelf flows to the slope could be an important mechanism in the carbon pump, as well as driving biological growth on the shelf in the case of troughs upwelling nutrient-rich waters from depths below ((Cape et al. 2019); Holt, Wakelin, and Huthnance 2009). Troughs enhancing the upwelling of slope currents to the shelf and subsequent concentration of these waters onshore into the fjord region is a heat-transfer mechanism responsible for glacial melt (Rysgaard et al. 2020; Walker et al. 2007; Wåhlin et al. 2013). Model results explored here show that troughs upwell flows along isobaths shallower than the deepest depths of the trough. The upwelling and subsequent of exchange of slope flows from depths below the trough must first be brought up by some other mechanism. Finally, as troughs cause currents to migrate offshore towards the slope, this will be one cause of the (often-observed) shelfbreak jet (Fratantoni and Pickart 2007; Greatbatch, Pal, and Ren 1995; Greenberg and Petrie 1988; Han et al. 2008). This may contribute to the insulation of coastal dynamics from basin-scale forcing (Chapman 1985).

This study shows that troughs can significantly impact coastal circulation. An increased understanding of how significantly the trough impact is will come as these results are applied to observations, and this study is expanded beyond these physical limits, i.e., the barotropic, linear, and steady-state dynamics explored here.

6 Appendix

6.1 Numerical Recipe

The model created for this study solves the vorticity equation (3) for a streamfunction Ψ, given input geometry and forcing conditions. A direct solver is constructed to solve this governing equation term by term over the entire domain. Terms are constructed where partial derivatives (H_x, H_y, Ψ_x, Ψ_y) are central derivatives (apart from domain edges). The alongshore and offshore resolutions of these terms are 500 and 100 meters, respectively. Terms generated are filled into a matrix of vorticity equations, which describe the entire domain.

All matrix filling and calculations steps are conducted in sparse form. This eliminates unnecessary computation of zeros, and it speeds up run times significantly. The boundary conditions, as prescribed in the methods, are handled in the matrix construction when domain edges are met. For runs where downwave winds exist, an array of alongshore wind stress values is constructed as a forcing term.

After these matrix constructions steps are done, a streamfunction is solved for with built-in linear algebra tools of Python. The streamfunction, Ψ, is found in this vector form and then transformed into domain space (x by y):

$$E\Psi = F, \tag{8}$$

where E is the N by N equation matrix (where N is equal to the total amount of grid cells of the domain), Ψ is an N by one streamfunction vector, and F is the forcing (which may include downwave winds).

6.2 Downwave Boundary Condition

The choice of downwave boundary condition is arbitrary to within an "error distance," upwave of it. This error distance is found by scaling the vorticity equation in the limit of the downwave boundary being a "no-flow," hard wall, eliminating alongshore transport, Ψ_x:

$$0 = J(\Psi, \frac{f}{H}) + \nabla(\frac{r}{H^2}\nabla\Psi) \Rightarrow \frac{\partial}{\partial y}(\frac{f}{H})\cancelto{0}{\Psi_x} + \frac{\partial}{\partial x}(\frac{f}{H})\Psi_y + \frac{\partial}{\partial x}(\frac{r}{H^2}\cancelto{0}{\Psi_x}) + \frac{\partial}{\partial y}(\frac{r}{H^2}\Psi_y) \qquad (9)$$

This leaves a vorticity balance whose alongshore length scale describes this upwave error distance. This is the distance upwave that flow adjusts to this wall, i.e., the upwave length that the wall "forces" the domain. This has been described previously as a frictional boundary layer, or Stommel width (Pringle 2002; Stommel 1948).

$$L_y = L_{fric} \propto \frac{r}{fH_x}, \qquad (10)$$

where Ψ_y scales as $\frac{\Psi}{L_y}$.

This limit case gives the maximum upwave extent of this adjustment. The baseline values used in this model give a frictional (Stommel) width of O(5 km), or about 1% of the alongshore distance. Therefore, the vast majority of this shelf system is unforced/unperturbed by this downwave boundary phenomenon.

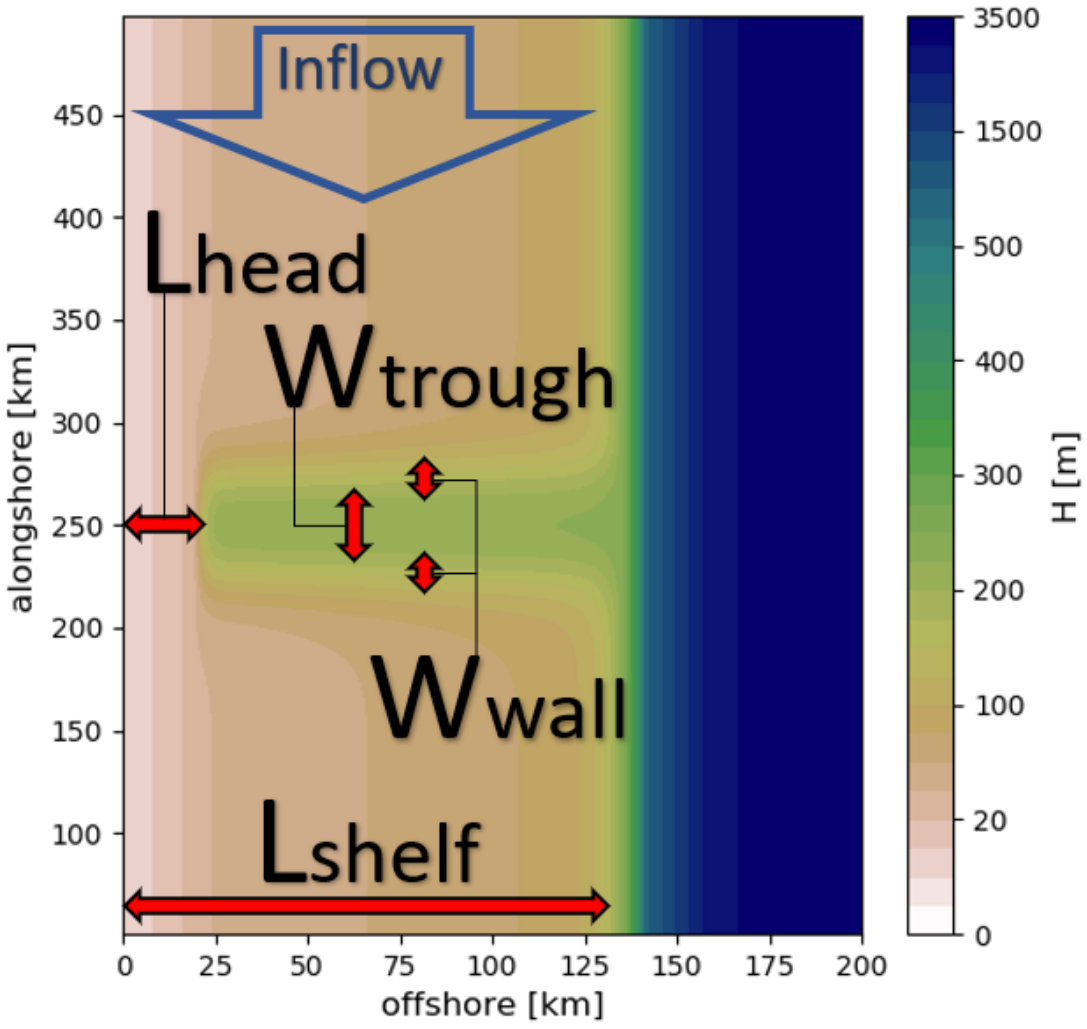

Figure 1: Model bathymetry includes a trough on the shelf. The key geometric parameters used in the scaling analysis are labeled with red cartoon arrows. The upwave forcing of wind-generated shelf flows are labeled with a blue cartoon arrow.

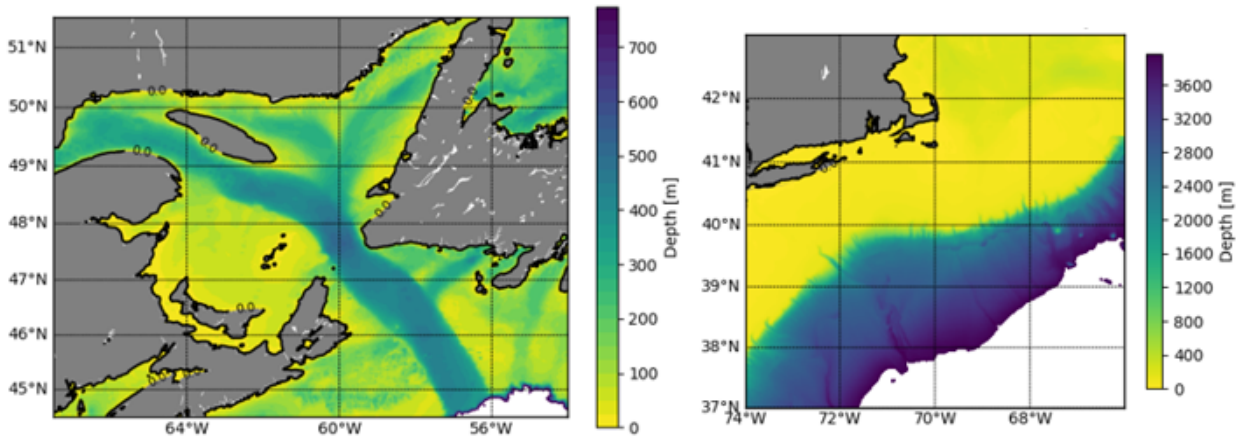

Figure 2: On the left is a bathymetry plot of the Laurentian Channel, which is a significant glacial trough that incises the shelf almost entirely. On the right is a bathymetry plot of the region southeast of Cape Cod, which is home to many river-carved canyons that incise mainly the slope. Notice the Hudson Canyon (39.5°N, 72°W) is exceptional because it incises the shelf. As a general principle, canyons incise the slope but not the shelf, contrarily to troughs which incise the shelf but not the slope.

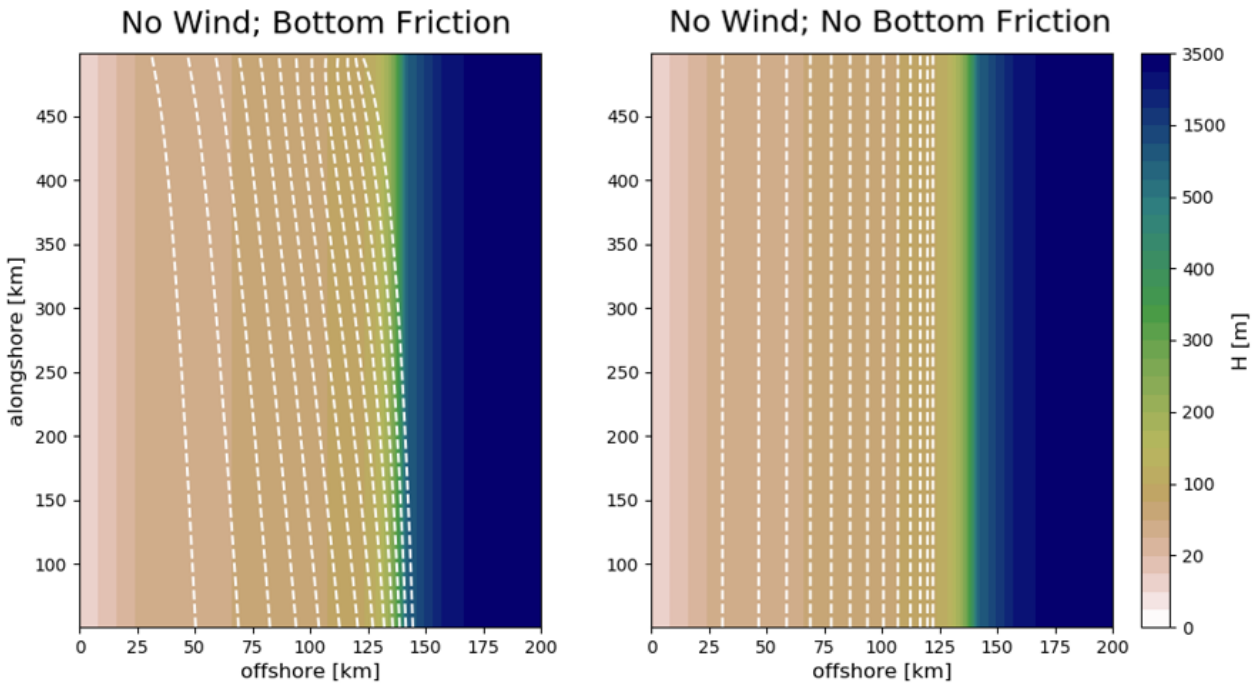

Figure 3: Streamlines are plotted as white dashed lines over color-coded bathymetry. On the left is a plot of a run with bottom friction, whereas on the right is one without bottom friction. Both runs were forced solely by wind-generated shelf flows that enter the upwave boundary, i.e., no winds within the domain.

Table 1: Model input parameters′ baseline values, as well as minima, maxima, and increments used in variation runs.

Parameter	Baseline value	Minimum[a]	Maximum[a]	Step Size[a]
$r[\frac{m}{s}]$	0.005	0.002	0.01	0.001
$f[\frac{1}{s}]$	0.001	0.0001	0.0015	0.0001
$H_{shelfbreak}[m]$	100	50	400	50
$H_{trough}[m]$	250	0	600	50
$L_{head}[km]$	20	0	150	10
$L_{shelf}[km]$	150	100	180	5
$W_{wall}[km]$	20	5	50	5
$W_{trough}[km]$	50	0	150	10

[a]Applies to the variation runs.

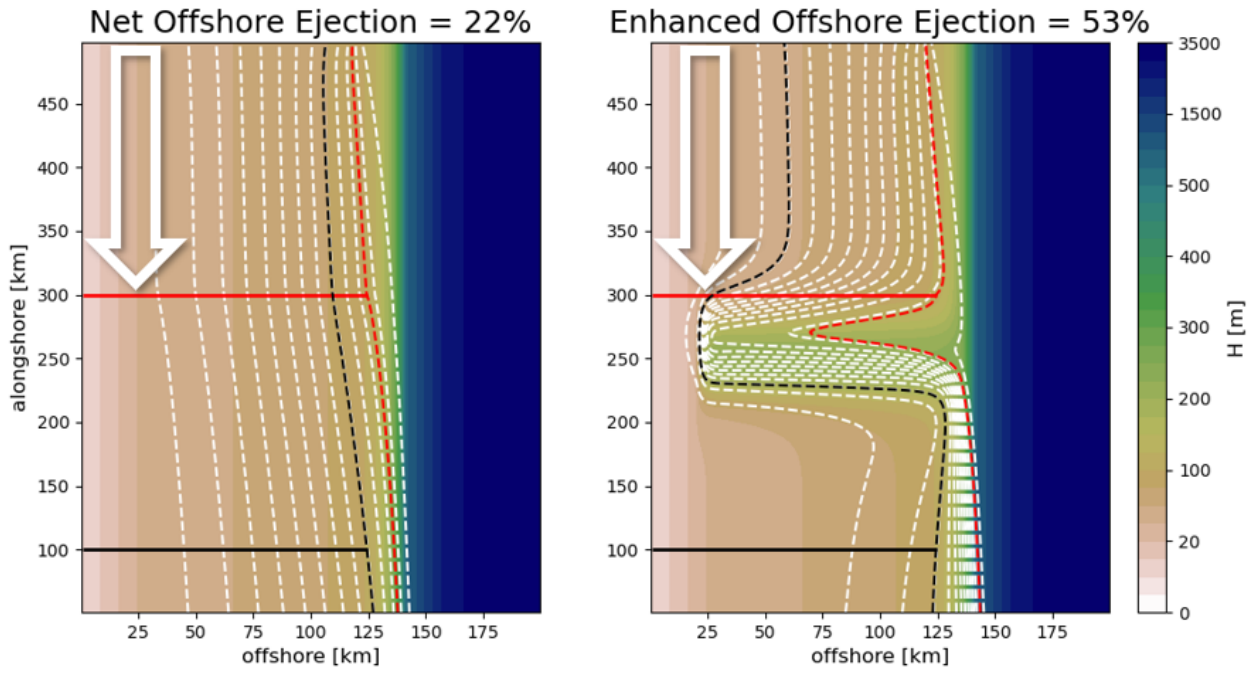

Figure 4: Resulting streamlines of two model runs are plotted as white dashed lines. On the left is of a run without a trough, and on the right is one with a baseline-parameter trough. White cartoon arrows are included to represent the shelf wind forcing, which is confined to only the shelf upwave of the trough location. Loss of shelf transport to the slope is quantified by calculating the difference in flow from the upwave (red) transect to the downwave (black) transect.

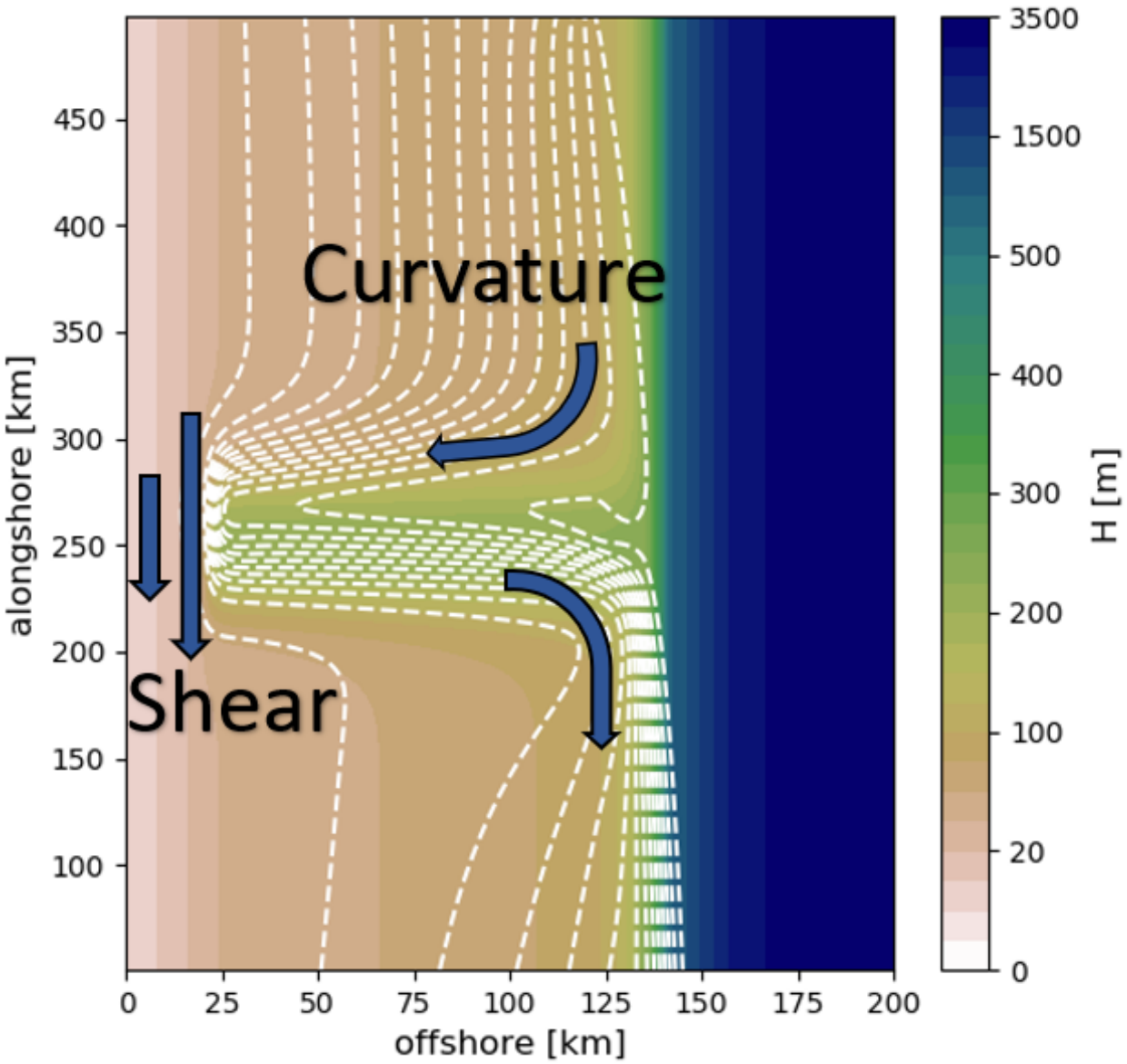

Figure 5: This baseline-parameter trough run is superimposed with blue cartoon arrows, representing the two relative vorticity sources: curvature and shear (narrowing).

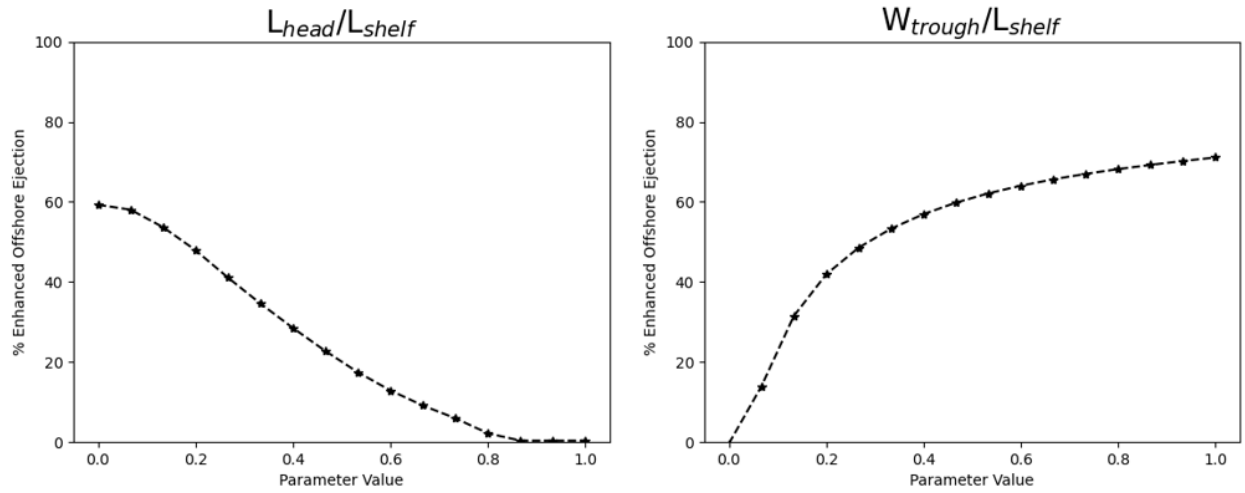

Figure 6: Two different parameter variation results are plotted here to show the impact of the narrowing source on offshore ejection, i.e., change in ejection as a function of parameter value change. On the left is the parameter $\frac{L_{head}}{L_{shelf}}$, which controls the magnitude of velocity shear, reaching a maximum as the shelf width narrows to zero, and reaching a minimum as the trough disappears to the slope. On the right is the parameter $\frac{W_{trough}}{L_{shelf}}$, which controls the accumulation of the shear impact. Ejection change is directly proportional to this parameter (trough width) because a longer alongshore distance allows for a higher accumulation of the shear impact. An O(1) change in both parameters alters offshore ejection by approximately 60%.

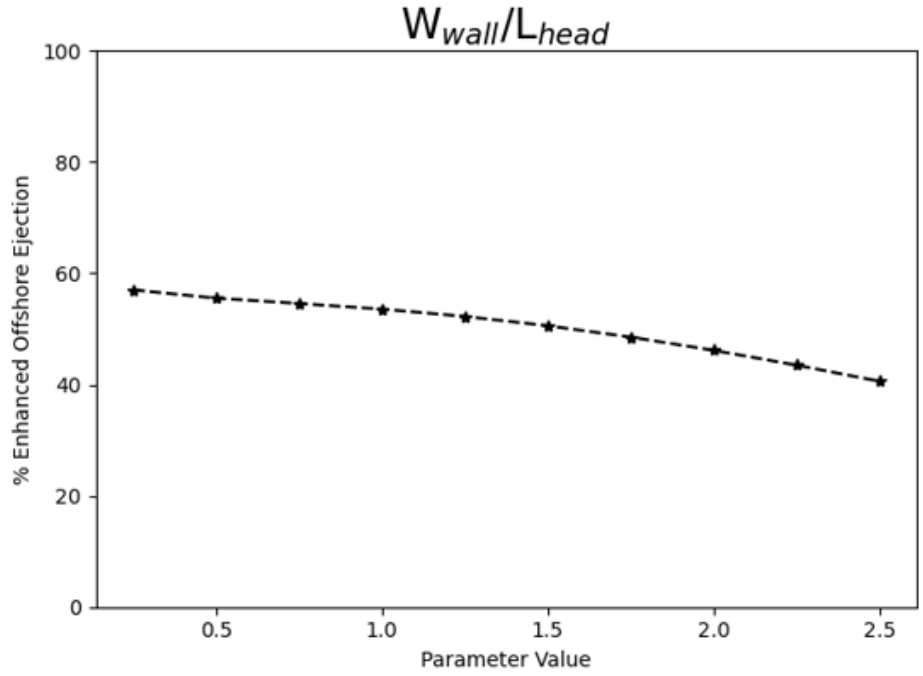

Figure 7: This parameter variation result shows the impact of the curvature source on offshore ejection. As the parameter $\frac{W_{wall}}{L_{head}}$ increases, the offshore ejection by the trough reduces. This is because the alongshore extent of the wall is increasing, i.e., more gradual walls, which reduces the significance of isobath curvature and therefore reduces the curvature impact on offshore ejection. Unlike the narrowing source's scaling, an O(1) change in this curvature parameter alters offshore ejection by approximately 10%, or one-fifth that of the narrowing source impact.

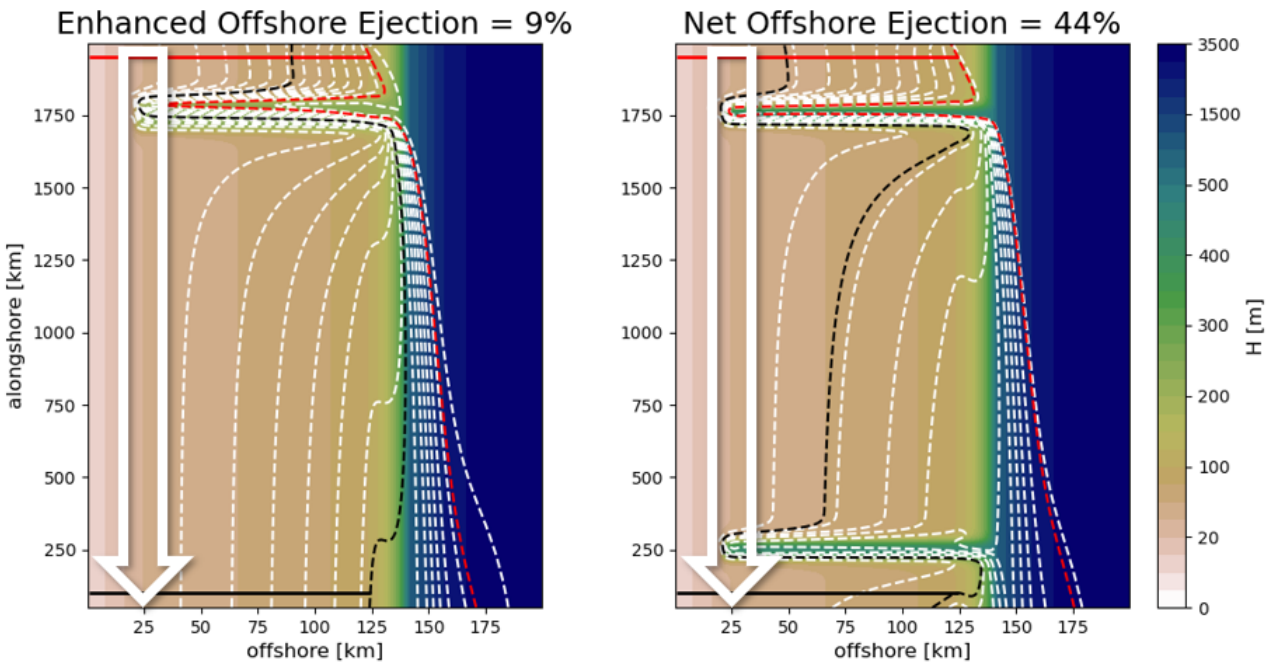

Figure 8: Resulting streamlines of two model runs are plotted above: one with a single trough (left) and one with two troughs (right). White cartoon arrows are included to represent the wind forcing, which extends over the entire shelf domain. Loss of shelf transport to the slope is quantified by calculating the difference in flow from the upwave (red) transect to the downwave (black) transect.

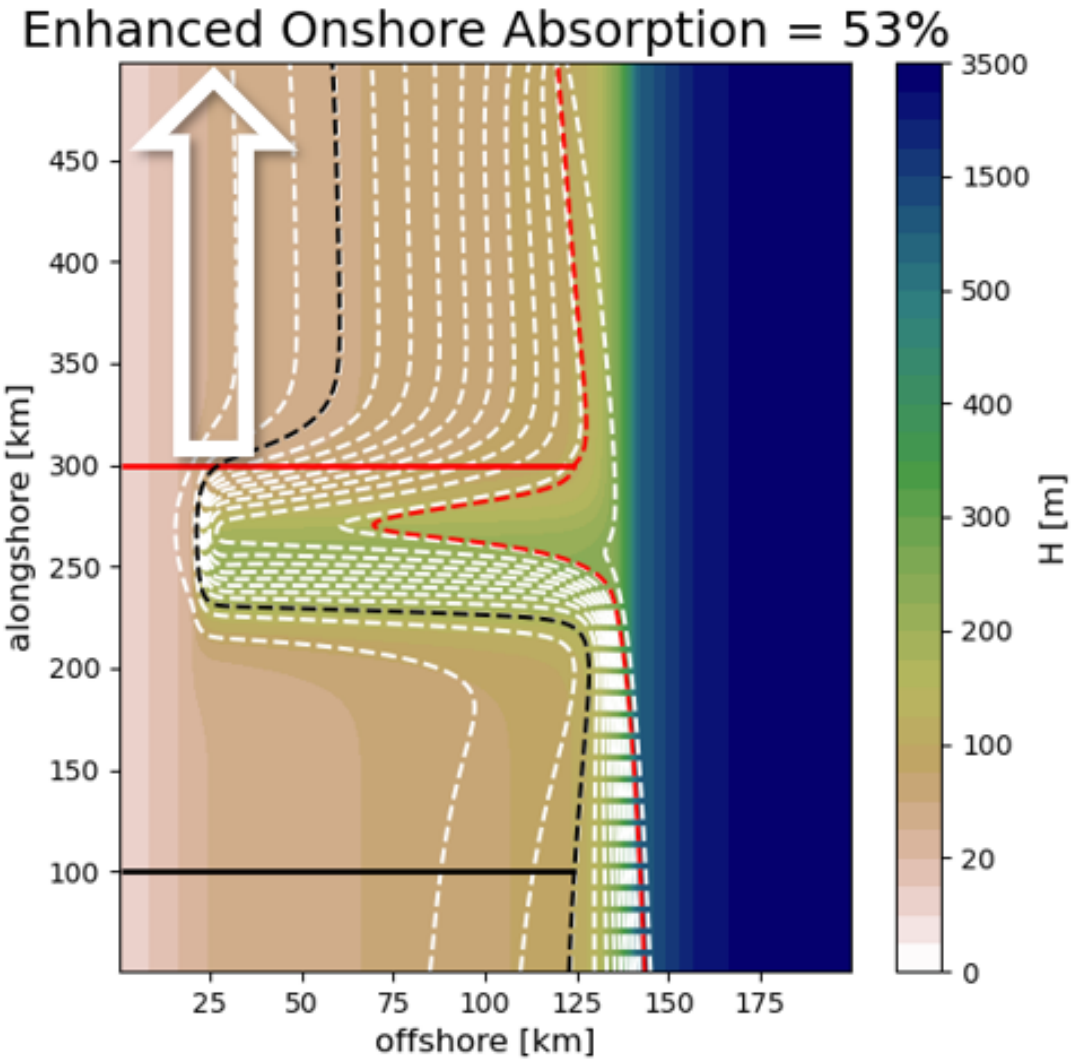

Figure 9: Resulting streamlines are contoured of a single-trough model run. A white cartoon arrow is included to represent the wind forcing. The percentage of slope transport absorbed onto the shelf is quantified by calculating the difference in flow from the downwave (black) transect to the upwave (red) transect.

7 References

Allen, Susan E. and Barbara M. Hickey (Aug. 2010). "Dynamics of advection-driven upwelling over a shelf break submarine canyon". In: *Journal of Geophysical Research: Oceans* 115.C8.

Battisti, David S. and Barbara M. Hickey (May 1984). "Application of Remote Wind-Forced Coastal Trapped Wave Theory to the Oregon and Washington Coasts". In: *Journal of Physical Oceanography* 14.5, pp. 887–903.

Beardsley, Robert C. and Dale B. Haidvogel (Mar. 1981). "Model Studies of the Wind-Driven Transient Circulation in the Middle Atlantic Bight. Part 1: Adiabatic Boundary Conditions". In: *Journal of Physical Oceanography* 11.3, pp. 355–375.

Brink, K. H. (Aug. 2006). "Coastal-trapped waves with finite bottom friction". en. In: *Dynamics of Atmospheres and Oceans* 41.3, pp. 172–190.

Brink, Kenneth H. and J. S. Allen (Sept. 1978). "On the Effect of Bottom Friction on Barotropic Motion Over the Continental Shelf". In: *Journal of Physical Oceanography* 8.5, pp. 919–922.

Buhl-Mortensen, Lene et al. (2012). "51 - Banks, Troughs, and Canyons on the Continental Margin off Lofoten, Vesterålen, and Troms, Norway". In: *Seafloor Geomorphology as Benthic Habitat*. Ed. by Peter T. Harris and Elaine K. Baker. London: Elsevier, pp. 703–715.

Cape, Mattias R. et al. (Jan. 2019). "Nutrient release to oceans from buoyancy-driven upwelling at Greenland tidewater glaciers". en. In: *Nature Geoscience* 12.1, pp. 34–39.

Chapman, David C. (Aug. 1985). "Numerical Treatment of Cross-Shelf Open Boundaries in a Barotropic Coastal Ocean Model". In: *Journal of Physical Oceanography* 15.8, pp. 1060–1075.

Chapman, David C. (July 1986). "A Simple Model of the Formation and Maintenance of the Shelf/Slope Front in the Middle Atlantic Bight". In: *Journal of Physical Oceanography* 16.7, pp. 1273–1279.

Chapman, David C. and Glen Gawarkiewicz (Sept. 2012). "Offshore transport of dense shelf water in the presence of a submarine canyon". In: *Journal of Geophysical Research: Oceans* 100.C7, pp. 13373–13387.

Csanady, G. T. (Jan. 1978). "The Arrested Topographic Wave". In: *Journal of Physical Oceanography* 8.1, pp. 47–62.

Dever, M. et al. (May 2016). "Hydrography and Coastal Circulation along the Halifax Line and the Connections with the Gulf of St. Lawrence". In: *Atmosphere-Ocean* 54.3, pp. 199–217.

Fratantoni, Paula and Robert Pickart (2007). "The Western North Atlantic Shelfbreak Current System in Summer". In: *Journal of Physical Oceanography* 10, p. 2509.

Gawarkiewicz, Glen and David C. Chapman (Aug. 1991). "Formation and Maintenance of Shelfbreak Fronts in an Unstratified Flow". In: *Journal of Physical Oceanography* 21.8, pp. 1225–1239.

Gordon, R. L. (1982). "Coastal ocean current response to storm winds". en. In: *Journal of Geophysical Research: Oceans* 87.C3, pp. 1939–1951.

Greatbatch, Richard J., Badal K. Pal, and Ying Ren (Jan. 1995). "Experiments using a long-time-scale shelf circulation model of relevance to the Labrador Current". In: *Continental Shelf Research* 15.1, pp. 41–57.

Greenberg, David A. and Brian D. Petrie (1988). "The mean barotropic circulation on the Newfoundland shelf and slope". en. In: *Journal of Geophysical Research: Oceans* 93.C12, pp. 15541–15550.

Han, Guoqi et al. (2008). "Seasonal variability of the Labrador Current and shelf circulation off Newfoundland". en. In: *Journal of Geophysical Research: Oceans* 113.C10.

Harris, Peter T. and Tanya Whiteway (July 2011). "Global distribution of large submarine canyons: Geomorphic differences between active and passive continental margins". In: *Marine Geology* 285.1, pp. 69–86.

Holt, Jason, Sarah Wakelin, and John Huthnance (2009). "Down-welling circulation of the northwest European continental shelf: A driving mechanism for the continental shelf carbon pump". en. In: *Geophysical Research Letters* 36.14.

Janowitz, Gerald S. and Leonard J. Pietrafesa (Nov. 1982). "The effects of alongshore variation in bottom topography on a boundary current—(topographically induced upwelling)". In: *Continental Shelf Research* 1.2, pp. 123–141.

Lentz, Steve et al. (1999). "Momentum balances on the North Carolina inner shelf". en. In: *Journal of Geophysical Research: Oceans* 104.C8, pp. 18205–18226.

Price, James F. (May 2003). "Dimensional analysis of models and data sets". en. In: *American Journal of Physics* 71.5, pp. 437–447.

Pringle, James M. (Nov. 2002). "Enhancement of Wind-Driven Upwelling and Downwelling by Alongshore Bathymetric Variability". In: *Journal of Physical Oceanography* 32.11, pp. 3101–3112.

— (2018). "Remote Forcing of Shelf Flows by Density Gradients and the Origin of the Annual Mean Flow on the Mid-Atlantic Bight". en. In: *Journal of Geophysical Research: Oceans* 123.7, pp. 4464–4482.

Rysgaard, S. et al. (2020). "An Updated View on Water Masses on the pan-West Greenland Continental Shelf and Their Link to Proglacial Fjords". en. In: *Journal of Geophysical Research: Oceans* 125.2, e2019JC015564.

Sandstrom, H. (1980). "On the wind-induced sea level changes on the Scotian shelf". en. In: *Journal of Geophysical Research: Oceans* 85.C1, pp. 461–468.

Stommel, Henry (1948). "The westward intensification of wind-driven ocean currents". en. In: *Eos, Transactions American Geophysical Union* 29.2, pp. 202–206.

Straneo, Fiammetta et al. (May 2011). "Impact of fjord dynamics and glacial runoff on the circulation near Helheim Glacier". en. In: *Nature Geoscience* 4.5, pp. 322–327.

Walker, Dziga P. et al. (Jan. 2007). "Oceanic heat transport onto the Amundsen Sea shelf through a submarine glacial trough". In: *Geophysical Research Letters* 34.2.

Wåhlin, A. K. et al. (May 2013). "Variability of Warm Deep Water Inflow in a Submarine Trough on the Amundsen Sea Shelf". In: *Journal of Physical Oceanography* 43.10, pp. 2054–2070.

Williams, William J and Eddy C. Carmack (Sept. 2008). "Combined effect of wind-forcing and isobath divergence on upwelling at Cape Bathurst, Beaufort Sea". In: *Journal of Marine Research* 66.5, pp. 645–663.

Williams, William J, Glen G Gawarkiewicz, and Robert C Beardsley (Jan. 2001). "The adjustment of a shelfbreak jet to cross-shelf topography". In: *Deep Sea Research Part II: Topical Studies in Oceanography*. Coupled biological and physical studies of plankton populations on Georges Bank and related North Atlantic regions 48.1, pp. 373–393.

Wright, Daniel G. and Keith R. Thompson (Feb. 1983). "Time-Averaged Forms of the Nonlinear Stress Law". In: *Journal of Physical Oceanography* 13.2, pp. 341–345.

Zhang, Weifeng (Gordon) and Steven J. Lentz (Dec. 2017). "Wind-Driven Circulation in a Shelf Valley. Part I: Mechanism of the Asymmetrical Response to Along-Shelf Winds in Opposite Directions". en. In: *Journal of Physical Oceanography* 47.12, pp. 2927–2947.